

Supplementary Information

Title: Specific ligand-receptor interactions govern binding and cooperativity of diverse modulators to a common metabotropic glutamate receptor 5 allosteric site

Karen J. Gregory^{1,2,3#}, Elizabeth D. Nguyen^{4#}, Chrysa Malosh^{1,2}, Jeffrey L. Mendenhall, Jessica Z. Zic^{1,2}, Brittney S. Bates^{1,2}, Meredith J. Noetzel^{1,2}, Emma F. Squire^{1,2}, Eric M. Turner^{1,2}, Jerri M. Rook^{1,2}, Kyle A. Emmitte^{1,2,5}, Shaun R. Stauffer^{1,2,5}, Craig W. Lindsley^{1,2,5}, Jens Meiler^{1,4,5,6*} and P. Jeffrey Conn^{1,2*}.

these authors contributed equally to this work.

¹Department of Pharmacology, Vanderbilt University Medical Center, Nashville, TN, USA.

² Vanderbilt Center for Neuroscience Drug Discovery, Vanderbilt University Medical Center, Nashville, TN, USA.

³ Drug Discovery Biology, Monash Institute of Pharmaceutical Sciences, Monash University, Parkville, VIC, Australia.

⁴ Center for Structural Biology, Vanderbilt University Medical Center, Nashville, TN, USA.

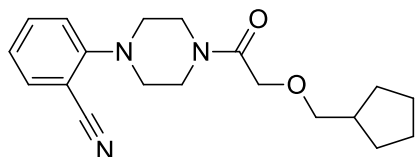
⁵ Department of Chemistry, Vanderbilt University Medical Center, Nashville, TN, USA.

⁶ Institute for Chemical Biology, Vanderbilt University Medical Center, Nashville, TN, USA.

* joint corresponding authors

Chemistry General Methods. Low resolution mass spectra were obtained on an Agilent 1200 series 6130 mass spectrometer. Analytical thin layer chromatography was performed on Analtech silica gel GF 250 micron plates. Analytical HPLC was performed on an HP1100 with UV detection at 214 and 254 nm along with ELSD detection, LC/MS (J-Sphere80-C18, 3.0 x 50 mm, 4.1 min gradient, 5%[0.05%TFA/CH₃CN]:95%[0.05%TFA/H₂O] to 100%[0.05%TFA/CH₃CN]. Preparative RP-HPLC purification was performed on a custom HP1100 automated purification system with collection triggered by mass detection or using a Gilson Inc. preparative UV-based system using a Phenomenex Luna C18 column (50 x 30 mm I.D., 5 mm) with an acetonitrile (unmodified)-water (0.1% TFA) custom gradient. Normal-phase silica gel preparative purification was performed using an automated Combi-flash companion from ISCO. Solvents for extraction, washing and chromatography were HPLC grade. All reagents were purchased from Aldrich Chemical Co. and were used without purification.

Preparation of 2-(4-(2-(cyclopentylmethoxy)acetyl)piperazin-1-yl)benzotrile 6I (VU0403038).



Step 1. 1-(2-Cyanophenyl)-piperazine (1.0 g, 4.93 mmol) and DIPEA (1.0 g, 7.8 mmol) were dissolved in CH₂Cl₂ (25 mL) and cooled to 0° C. To this solution chloroacetyl chloride (0.67 g, 5.92 mmol, 1.2 eq) dissolved in CH₂Cl₂ (5 mL) was added slowly over 10 min. The reaction was allowed to warm to room temperature and stir for 2h. The mixture was poured onto aq. NaHCO₃ (20 mL) and brine (10 mL). The mixture was extracted with EtOAc (3 x 20 mL) and the combined organic layers dried over Na₂SO₄, filtered, and the volatiles removed. The residue was purified on silica gel, eluted with EtOAc in hexanes (0-70%) to give 2-(4-(2-chloroacetyl)piperazin-1-yl)benzotrile (0.9 g, 69% yield) as an off-white semi-solid. The residue was used directly in Step 2.

Step 2. To a solution of cyclopentylmethanol (131 mg, 0.4 mmol) in DMF (1.0 mL) was added NaH (95%, 7.5 mg) and stirred for 40 min. A separate DMF (1.0 mL) solution charged with 2-(4-(2-chloroacetyl)piperazin-1-yl)benzotrile (53 mg, 0.2 mmol) from Step 1 was added to the NaH/DMF suspension and heated at 70 °C for 3h. The mixture was cooled to rt and poured onto H₂O (5 mL). The mixture was extracted with EtOAc (2 x 10 mL). The combined extracts were treated with brine, dried over Na₂SO₄, filtered, and the volatiles removed under reduced pressure. Purification using RP-HPLC afforded title compound 2-(4-(2-(cyclopentylmethoxy)acetyl)piperazin-1-yl)benzotrile as an off-white solid (22 mg, 35%): LC-MS (*m/z*) = 328.2 [M+H], >98% (215 nm, ELSD), Rt = 3.30 min.

Docking of allosteric ligands into the mGlu₅ comparative model

The initial ligand docking experiments started at a manually placed position centered at P654, which was chosen given that mutations at this residue impacted each of the modulators (Fig. 1). Ligand docking of 42 active modulators proceeded as previously described (1). After generating 5,000 models of mGlu₅-ligand complexes during the first ligand docking round, the top 10% of models by ligand interaction energy were carried on to a second round as described above. During the second docking round, the starting binding mode from the model generated in the first round was used rather than manual assignment. After generating 5,000 models during the second round, the top 10% of models were again used to seed a third round. After the third docking set, the top 10% of models were clustered based on ligand root mean square deviation (RMSD) with a cutoff of 3 Å (2) and the center of each cluster with more than 2 members was used for further analysis.

Docking non-functional ligands into the mGlu₅ comparative model

Three inactive (or very low potency) compounds were chosen from each series to dock within the mGlu₅ comparative model. In doing so, top binding modes for active and inactive compounds could be compared and key structural elements that contribute to activity identified. The chosen inactive compounds are still able to bind the receptor; however, they elicit such a low response of glutamate modulation in intracellular Ca²⁺ mobilization studies that they are considered ineffective. Therefore, we docked them to the mGlu₅ receptor under the hypothesis that they must bind in a different, less effective binding mode than their active counterparts. As with the set of active ligands, inactive ligands were computationally docked into the comparative model of mGlu₅ using Rosetta Ligand (3-5). The ligands started at the position occupied by the top binding mode from their scaffold. Each modulator was allowed to sample binding modes in a 5.0 Å radius and full rotational freedom. After generating 5,000 models, the top 10% of models were clustered based on ligand root mean square deviation (RMSD) with a cutoff of 3 Å (2) and the center of each cluster with more than 2 members was used for further analysis.

Analysis of docking results within and across ligand scaffolds based on structure and atom properties

After three rounds of iterative ligand docking, the final binding modes from each of the 42 active modulators were compared within and across their scaffolds. Within each of the six scaffolds, cluster centers were compared against each other with a new measure called PropertyRMSD. This new measure distinguishes between common binding modes across different ligands of the same scaffold, aligning ligand atoms in space as well as aligning any user-defined atom properties. The measure is based loosely on the equation for RMSD₁₀₀, which normalizes the root mean square deviation between pairs of three-dimensional structures of different sizes (6). The equation has been modified as appropriate for ligands as such:

$$\text{Property RMSD}_N = \frac{\text{PRMSD}}{1 + a \cdot \log \frac{N}{B}}$$

where B is the number of atoms the user has specified should be aligned for a given pair of ligands, N is the actual number of atoms aligned, and a is computed such that the denominator equals 1/B at N = 1, to prevent non-physical (negative or infinite) RMSDs.

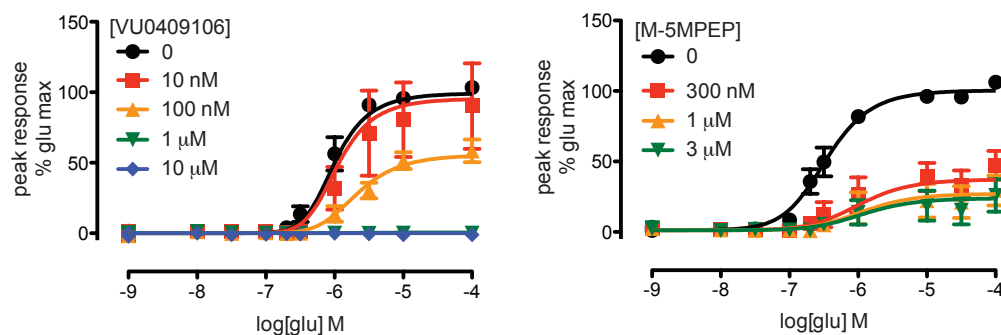
PRMSD is equivalent to the traditional formula for RMSD, but has been extended by distance between properties, e.g.

$$\text{PRMSD} = \sqrt{\sum_{n=1}^N (x_{1,n} - x_{2,n})^2 + (y_{1,n} - y_{2,n})^2 + (z_{1,n} - z_{2,n})^2 + \sum_i b_i (p_{i,1,n} - p_{i,2,n})^2}$$

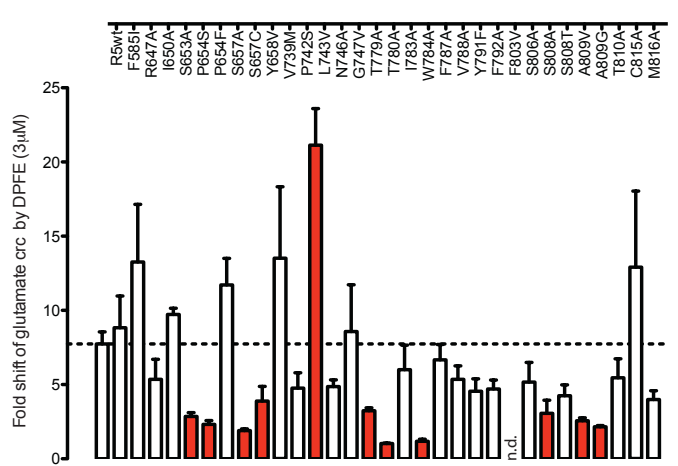
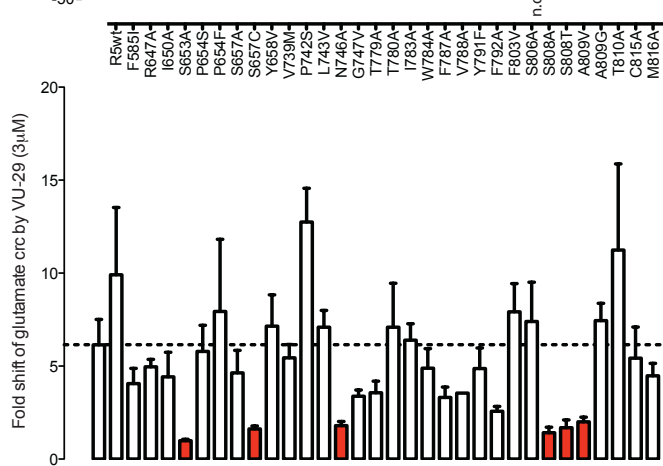
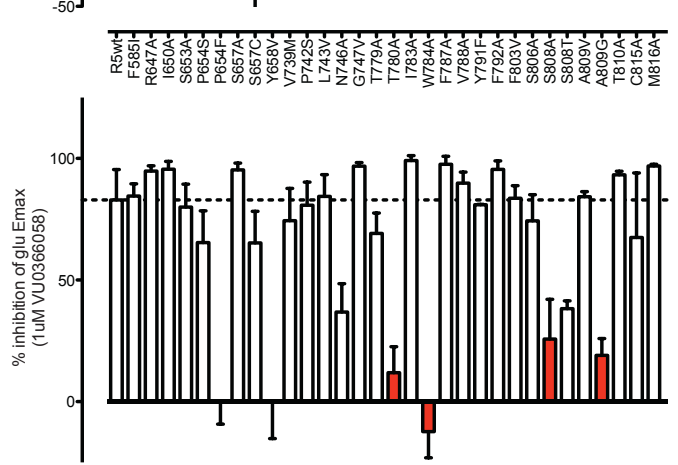
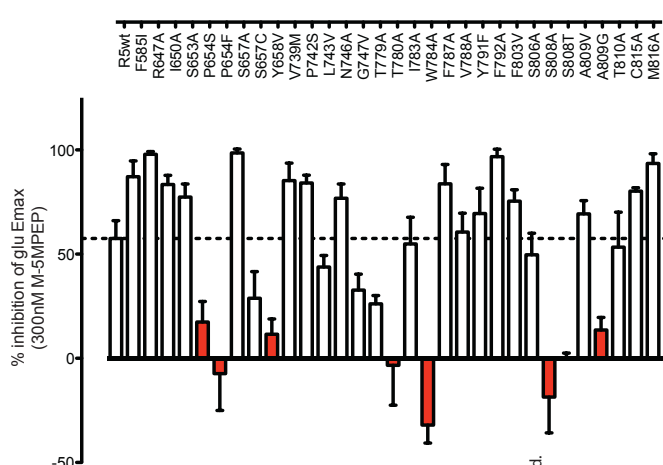
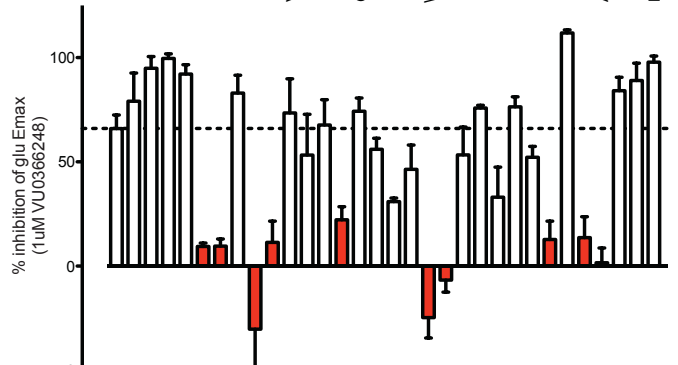
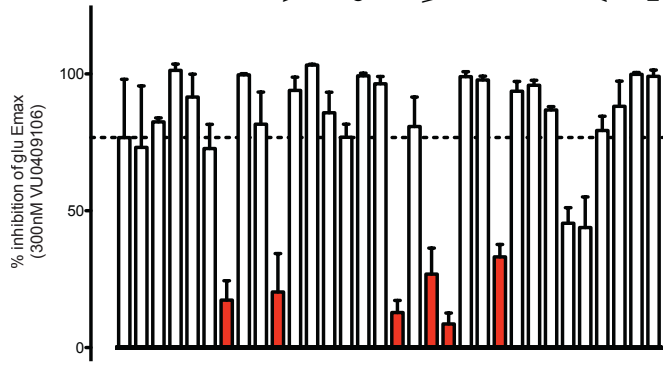
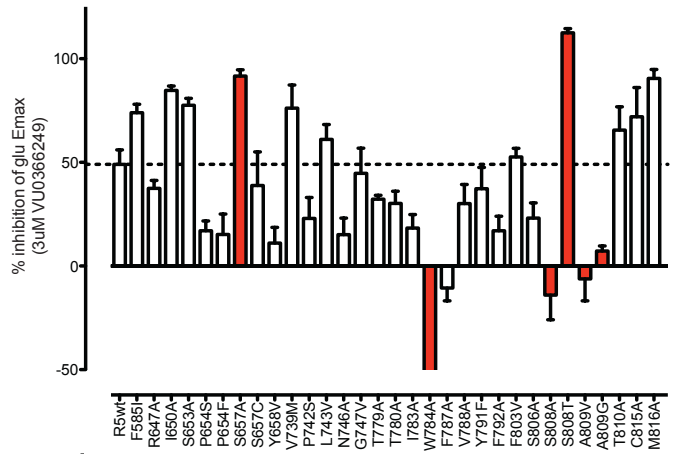
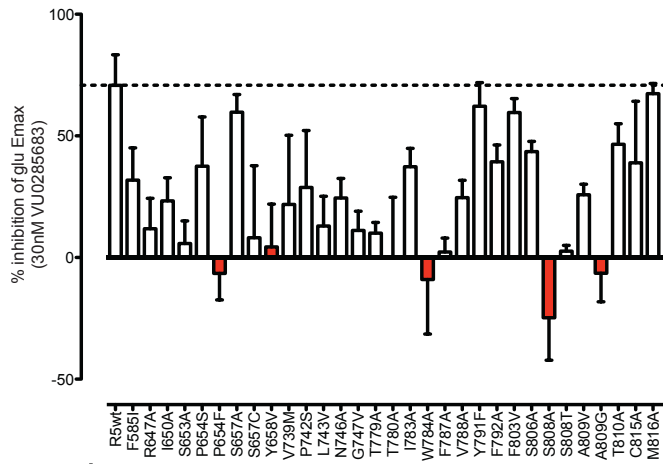
where $x_{1,n}$ refers to the x-position of the n-th atom on the first molecule, $x_{2,n}$ refers to the second molecule, etc. $p_{i,1,n}$ refers to the i-th property value of interest for atom n on the first molecule; b_i is an adjustable, property-dependent constant with units 1/A that is used to adjust for the ranges of various properties and the relative penalty for difference in distance versus property.

Binding mode analysis of five ligands from VU0366058 ligand series was used to benchmark the usage of the PropertyRMSD value compared to clustering with traditional RMSD. For the top 266 binding modes over

the 5 ligands in the series, traditional RMSD, PropertyRMSD with van der Waals volume alone, PropertyRMSD with sigma bond atomic charge alone and PropertyRMSD with the product of sigma bond atomic charge and van der Waals volume was evaluated and used to cluster the ligands with a cutoff of 1 unit. The largest cluster using each RMSD value was visually analysed, as seen in Supplementary Figure 4. The PropertyRMSD value using the product of sigma bond atomic charge and van der Waals volume, which we have named ChargeRMSD, was found to superimpose the ligand properties most accurately and was applied to this work. The value b_i was set to 5, which was the inverse standard deviation of this property over the ensemble of molecules. Once pairwise ChargeRMSD values were calculated for all ligands within a particular scaffold, the ligands were clustered with a cutoff of 1 unit and the largest 5 clusters, representing the most common binding modes within a particular scaffold, were further evaluated.

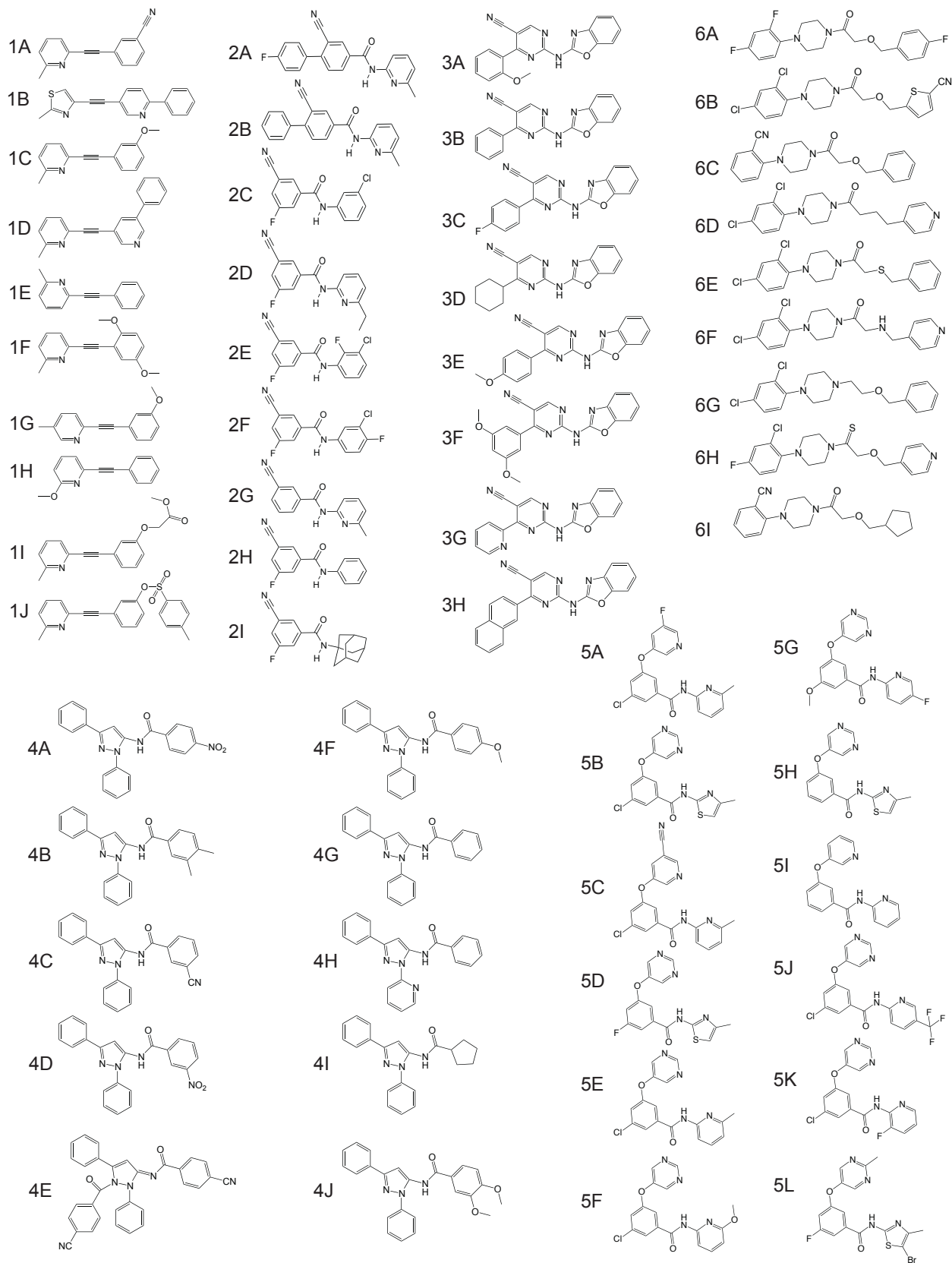


Supplementary Figure 1: Allosteric modulation of glutamate-mediated intracellular calcium release
HEK293A cells expressing mGlu₅ were exposed to different concentrations of indicated allosteric modulators for 1 min prior to performing a glutamate concentration-response curve. Data represent the mean±s.e.m of a minimum of three independent experiments performed in duplicate. Error bars not shown fall within the dimensions of the symbol.

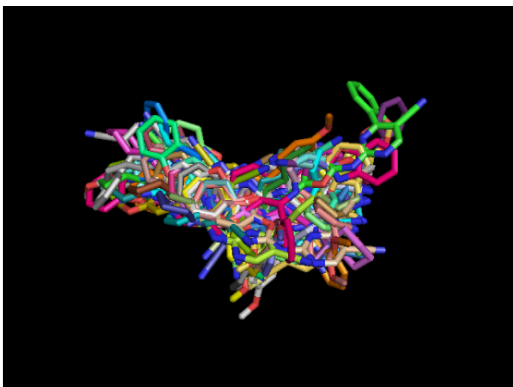
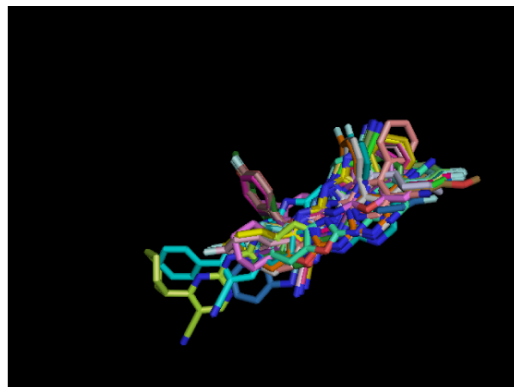
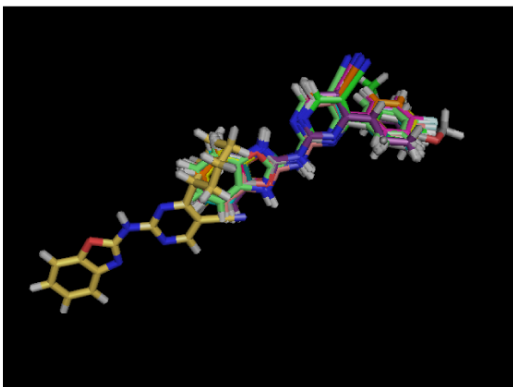
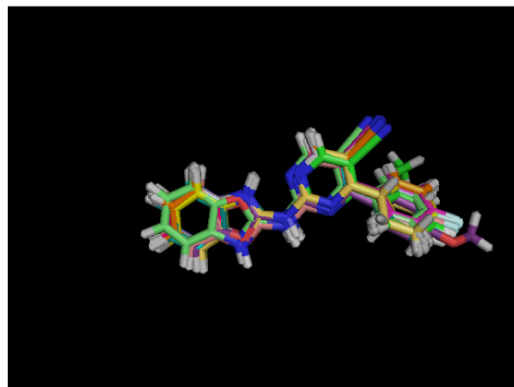


Supplementary Figure 2: Single concentration screen of allosteric modulators across all putative and known mutations within the common allosteric site

HEK293A cells expressing mGlu₅ were exposed to a single concentration of modulator (see y-axis) for 1 min prior to performing a glutamate-concentration response curve for intracellular calcium mobilization. The percent change in the maximal glutamate response in presence of NAMs is plotted. For PAMs, the change in glutamate potency in presence of PAM (fold-shift) is plotted. Red bars are significantly different to wildtype, one-way ANOVA, $p < 0.05$; n.d. indicates not determined. Data represent the mean \pm s.e.m of a minimum of three independent experiments performed in duplicate. Error bars not shown fall within the dimensions of the symbol.

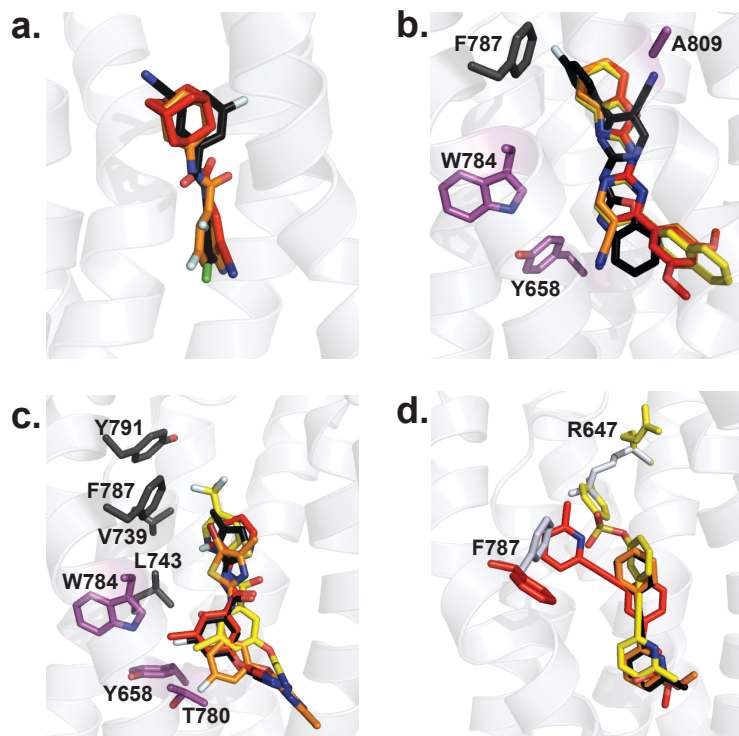


Supplementary Figure 3: Structures of allosteric ligands docked into the comparative model to sample SAR

a.**b.****c.****d.**

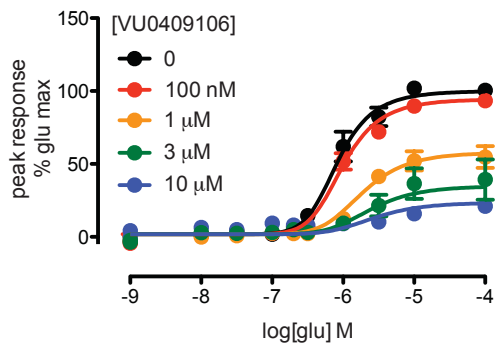
Supplementary Figure 4: Evaluation of PropertyRMSD over the VU0366058 ligand series

For the top 266 binding modes over 5 ligands in the VU0366058 ligand series, the largest cluster with a cutoff of 1 unit using a) traditional RMSD, b) PropertyRMSD with van der Waals volume alone, c) PropertyRMSD with sigma bond atomic charge alone and d) PropertyRMSD with the product of sigma bond atomic charge and van der Waals volume (named ChargeRMSD) is shown.



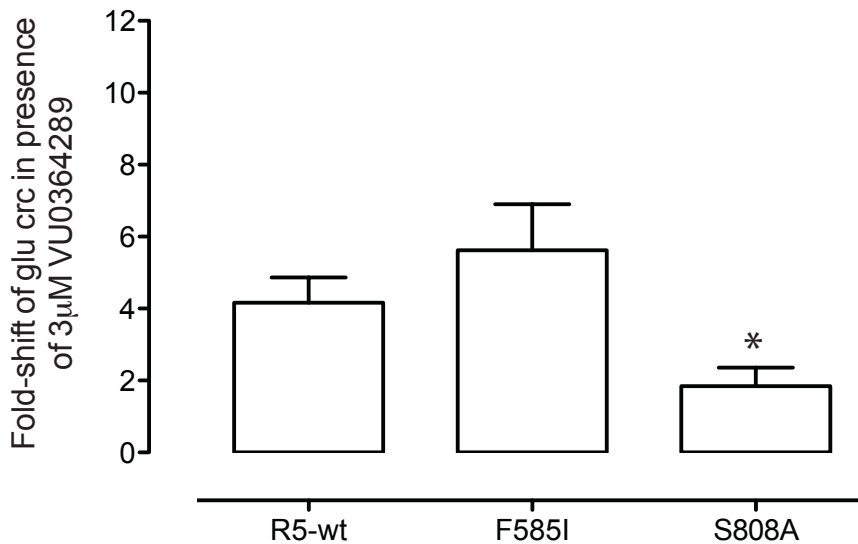
Supplementary Figure 5: Docking of inactive or low potency NAMs to mGlu5 comparative model to sample SAR

Docking of inactive compounds strengthened conclusions regarding the impact of mutations on allosteric modulator binding to the common allosteric site. a) Low potency or inactive compounds in the N-aryl benzamide series either lack polarity or have too little/much bulk on ring A; docking revealed these are generally found in the reverse, less favored, orientation, with the 3-cyano group buried: 2E (VU0366248) in black, 2H in orange and 2I in red. b) Similarly, for N-aryl-5-cyanopyrimidines the less favored buried position of the cyano group and deviation away from residues important for VU0366058 affinity was observed: 3C (VU0366058) in black, 3F in orange, 3G in red and 3H in yellow. c) Inactives in the aryl ether benzamide series, 5D (VU0409106) in black, 5J in orange, 5K in red and 5L in yellow, introduce bulk (e.g. 5L) or polarity (e.g. 5J and 5K) onto ring B. Introduction of the bromine atom in 5L forces the compound lower, likely disrupting desirable interactions with Y658, T780 and W784. d) Docking of inactive acetylene compounds (1E (MPEP) in black, 1H in orange, 1I in red and 1J in yellow) revealed substantial re-orientation of binding pocket residues is required to accommodate the large substitutions of the B ring (F787 for 1I and R647 for 1J). The methoxy substituent on ring A (1H) did not result in a markedly different binding mode; however, this substitution may obscure the pyridine interaction with S808.



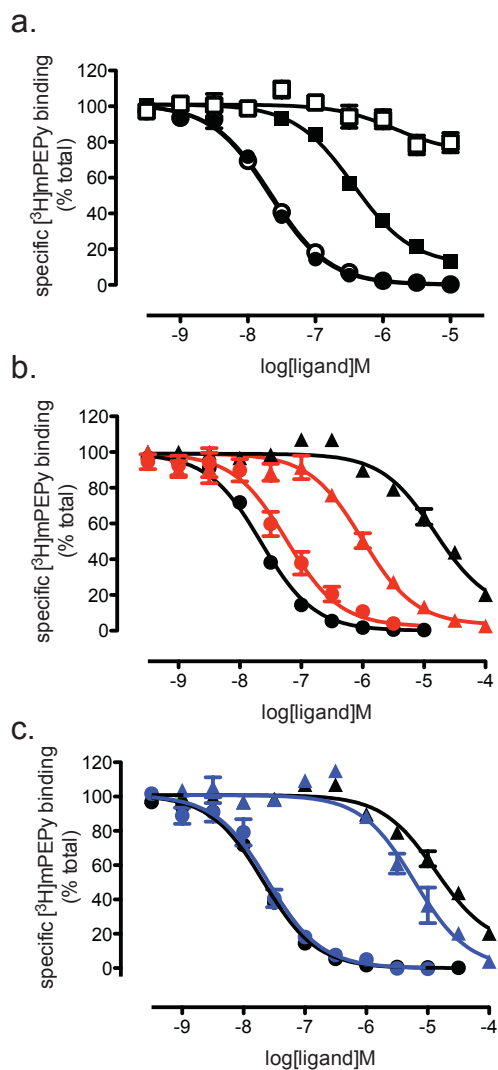
Supplementary Figure 6: W784A decreases the cooperativity of VU0409106.

HEK293A cells expressing mGlu₅-W784A were exposed to different concentrations of VU0409106 for 1 min prior to performing a glutamate concentration-response curve. Data represent the mean±s.e.m of a minimum of three independent experiments performed in duplicate. Error bars not shown lie within the dimensions of the symbol.



Supplementary Figure 7: VU0364289 an *N*-aryl piperazine PAM is sensitive to S808A

HEK293A cells expressing mGlu₅ mutants were exposed to 3μM of VU0364289 for 1 min prior to performing a glutamate concentration-response curve. The change in glutamate potency in the presence of PAM (fold-shift) is plotted. Data for R5-wt and F585I were previously reported in (7) and represent the mean±s.e.m of a minimum of three independent experiments performed in duplicate. * denotes significantly different to wild-type, one-way ANOVA with Dunnett's post-test.



Supplementary Figure 8: Inhibition of [³H]methoxyPEPy binding at wild type and mutant constructs. HEK293A cell membranes were equilibrated with ~2nM [³H]methoxyPEPy and varying concentrations of indicated allosteric ligands. **a**) Inhibition curves for MPEP (circles) and VU29 (squares) at wildtype (closed symbols) and G747V (open symbols). **b**) Inhibition curves for MPEP (circles) and DPFE (triangles) at wildtype (black) and L743V (red). **c**) Inhibition curves for MPEP (circles) and DPFE (triangles) at wildtype (black) and V788A (blue). [³H]-3-methoxy-5-(pyridin-2-ylethynyl)pyridine ([³H]methoxyPEPy; 76.3 Ci/mmol) was custom synthesized by PerkinElmer Life and Analytical Sciences (Waltham, MA). Radioligand binding assays were performed on HEK293A cell membranes as described previously (8). Binding affinity estimates (K_I) were derived using the Cheng-Prusoff method (9) or by applying the allosteric ternary complex as appropriate. Data represent the mean \pm s.e.m of a minimum of three independent experiments performed in duplicate. Error bars not shown fall within the dimensions of the symbol.

Supplementary Table 1: Summary of affinity estimates for allosteric modulators across selected point mutations. Data represent the mean±s.e.m of a minimum of three independent experiments performed in duplicate, unless otherwise indicated.

mutant	MPEP [#]	M-5MPEP	VU0366058	VU0285683	VU0409106	VU0366248	VU0366249	VU29	DPFE
R5-wt	8.58±0.17	7.03±0.16	6.66±0.25	7.50±0.21	7.19±0.16	6.70±0.04	6.44±0.15	6.87±0.19	5.85±0.14
P654F	4.11±0.21*	<4.5	No NAM	n.d.	5.79±0.25				
P654S	7.10±0.06*	5.55±0.28*	6.36±0.32	6.59±0.23	7.01±0.22	5.55±0.22*	<5	6.46±0.18	4.89±0.21*
S657C	8.32±0.08	6.65 ^b	n.d.	n.d.	n.d.	5.49±0.35*	6.38±0.14	n.d.	n.d.
S657A	8.80±0.06	7.58±0.19	n.d.	n.d.	n.d.	7.16±0.09	7.04 ^b	n.d.	n.d.
Y658V	6.57±0.13*	<4.5	5.07±0.26*	6.29±0.27*	5.78±0.13*	5.16±0.18*	No NAM	7.00±0.30	5.07±0.21*
P742S	8.07±0.17	6.55±0.09	n.d.	7.47±0.24	n.d.	n.d.	No NAM	6.47±0.01	4.43 ^{b*}
L743V	8.04±0.10	n.d.	n.d.	n.d.	n.d.	n.d.	n.d.	6.50±0.12	7.06±0.16*
N746A	8.30±0.06	6.55±0.22	6.66±0.25	6.75±0.10	6.01±0.07*	5.41±0.24*	<5	n.d.	n.d.
G747V	7.93±0.11*	7.03±0.11	7.43±0.13	7.63±0.17	7.21±0.16	7.09±0.19	7.03±0.16	5.40±0.26*	6.10±0.19
T780A	7.36±0.02*	6.55±0.14	6.69±0.20	6.48±0.14*	6.28±0.07*	6.13±0.07	<5	5.98±0.23*	4.00±0.39*
W784A	5.50±0.29*	No NAM	5.57±0.33*	5.14±0.28*	6.37±0.28*	5.59±0.26*	6.44±0.10	7.74±0.14	4.66±0.12*
F787A	6.80±0.04*	6.73±0.21	7.79±0.14*	5.51±0.20*	5.85±0.10*	No NAM	No NAM	6.57±0.19	5.77±0.09
V788A	7.89±0.17*	7.06±0.25	7.40±0.12	7.70±0.08	7.50±0.11	6.41±0.12	7.34±0.34*	6.52±0.09	6.99±0.29*
Y791A ^a	7.14 ^{*a,b}	6.72 ^{a,b}	7.34 ^{*a,b}	6.65 ^{*a,b}	6.22 ^{*a,b}	5.09 ^{*a,b}	4.24 ^{*a,b}	6.57±0.23	6.36±0.11
F792A	8.93±0.04	n.d.	n.d.	n.d.	6.70±0.27	6.56±0.20	n.d.	7.38±0.28	6.41±0.41
S808A	6.98±0.18*	4.61±0.24*	5.94±0.18	6.49±0.20*	7.31±0.13	5.67±0.28*	No NAM	7.02±0.17	5.39±0.09
S808T	6.90±0.06*	5.27±0.09*	6.49±0.26	6.17±0.27*	6.30±0.34*	7.56±0.17*	6.87±0.20	6.70±0.29	5.56±0.12
A809V	6.52±0.12*	6.71±0.21	6.28±0.21	6.82±0.18	5.82±0.25*	5.26±0.13*	No NAM	5.31±0.26*	5.04±0.16*
A809G	7.18±0.04*	5.39±0.32*	5.55±0.15*	6.38±0.14*	6.93±0.12	5.73±0.08*	No NAM	5.80±0.17*	4.82±0.09*

n.d. denotes not determined; based on the single point screen data, only significant mutations underwent the more rigorous analysis to determine affinity and cooperativity, using the operational model of allostery.

* denotes significantly different to wild type value, $p < 0.05$, using one-way ANOVA with Dunnett's post-test or t-test as appropriate.

[#] MPEP data (with the exception of S657A, F787A and Y791A) were reported previously (1) and are provided for reference.

^a Y791A had a very low signal in response to glutamate prohibiting determination of NAM effects. Thus, this construct was evaluated using [³H]methoxyPEPy binding assays and pK_I values are reported from $n=2$ independent experiments performed in triplicate and were compared to wild-type binding affinity estimates: MPEP = 8.02±0.04; M-5MPEP = 6.89±0.16; VU0366058 = 6.92±0.06; VU0285683 = 7.68±0.04; VU0366248 = 6.18±0.06; VU0366249 = 5.55±0.08 as reported previously (1, 8) and VU0409106 = 7.32±0.03.

^b data are mean of $n=2$.

Mutations of the six common determinant residues are highlighted in bold.

Supplementary References

1. Gregory, K. J., Nguyen, E. D., Reiff, S. D., Squire, E. F., Stauffer, S. R., Lindsley, C. W., Meiler, J., and Conn, P. J. (2013) Probing the metabotropic glutamate receptor 5 (mGlu(5)) positive allosteric modulator (PAM) binding pocket: discovery of point mutations that engender a "molecular switch" in PAM pharmacology, *Mol Pharmacol* 83, 991-1006.
2. Alexander, N., Woetzel, N., and Meiler, J. (2011) Bcl :Cluster: A method for clustering biological molecules coupled with visualization in the Pymol Molecular Graphics System, In *Proceedings of the 2011 IEEE 1st International Conference on Computational Advances in Bio and Medical Sciences*, pp 13-18, IEEE Computer Society.
3. Davis, I. W., and Baker, D. (2009) RosettaLigand docking with full ligand and receptor flexibility, *J Mol Biol* 385, 381-392.
4. Lemmon, G., and Meiler, J. (2012) Rosetta Ligand docking with flexible XML protocols, *Methods Mol Biol* 819, 143-155.
5. Meiler, J., and Baker, D. (2006) ROSETTALIGAND: protein-small molecule docking with full side-chain flexibility, *Proteins* 65, 538-548.
6. Carugo, O., and Pongor, S. (2001) A normalized root-mean-square distance for comparing protein three-dimensional structures, *Protein Sci* 10, 1470-1473.
7. Gregory, K. J., Herman, E. J., Ramsey, A. J., Hammond, A. S., Byun, N. E., Stauffer, S. R., Manka, J. T., Jadhav, S., Bridges, T. M., Weaver, C. D., Niswender, C. M., Steckler, T., Drinkenburg, W. H., Ahnaou, A., Lavreysen, H., Macdonald, G. J., Bartolome, J. M., Mackie, C., Hrupka, B. J., Caron, M. G., Daigle, T. L., Lindsley, C. W., Conn, P. J., and Jones, C. K. (2013) N-aryl piperazine metabotropic glutamate receptor 5 positive allosteric modulators possess efficacy in pre-clinical models of NMDA hypofunction and cognitive enhancement, *J Pharmacol Exp Ther.* 347, 438-457.
8. Gregory, K. J., Noetzel, M. J., Rook, J. M., Vinson, P. N., Stauffer, S. R., Rodriguez, A. L., Emmitte, K. A., Zhou, Y., Chun, A. C., Felts, A. S., Chauder, B. A., Lindsley, C. W., Niswender, C. M., and Conn, P. J. (2012) Investigating mGlu5 Allosteric Modulator Cooperativity, Affinity and Agonism: Enriching Structure-function Studies and Structure-activity Relationships, *Mol Pharmacol.* 82, 86-875.
9. Cheng, Y., and Prusoff, W. H. (1973) Relationship between the inhibition constant (K₁) and the concentration of inhibitor which causes 50 per cent inhibition (I₅₀) of an enzymatic reaction, *Biochemical Pharmacol* 22, 3099-3108.